

Synthesis of Side-Chain Liquid Crystalline Homopolymers and Block Copolymers with Cyanobiphenyl Moieties as the Mesogen by Living Anionic Polymerization and Their Thermotropic Phase Behavior

Masayuki Yamada, Tomomichi Itoh, Ryuta Nakagawa, Akira Hirao, Sei-ichi Nakahama, and Junji Watanabe*

Department of Polymer Chemistry, Tokyo Institute of Technology, Ookayama, Meguro-ku, Tokyo 152, Japan

Received August 28, 1998; Revised Manuscript Received November 18, 1998

ABSTRACT: We performed the anionic living polymerization of 6-[4-(4'-cyanophenyl)phenoxy]hexyl methacrylate. By a selection of suitable initiations, the cyano group was completely stable toward the propagating enolate anion, and the anionic polymerization proceeded with a living nature. The homopolymers could thus be prepared with a wide range of molecular weights from 6000 to 20 000, a narrow molecular weight distribution of less than 1.14, and different tacticities. All the polymers exhibited the smectic A phase in which two mesogenic groups were included within a smectic layer of thickness 36.0 Å. The isotropization temperature of the smectic A phase increased with the increase of the molecular weight and leveled off at around 15 000. No crystallization took place so that the smectic A phase was glassified. Well-controlled block copolymers with methyl methacrylate and styrene were also prepared by living anionic polymerization, and their thermotropic phase behavior and structures are described in a relation to a microphase separation of the two different segments.

1. Introduction

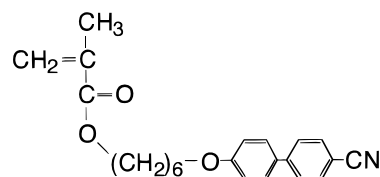
In recent years, research interests in side-chain liquid crystal polymers have focused mainly on the role of the main-chain backbone on the liquid crystal properties. There are many parameters with respect to the main-chain backbone such as a degree of polymerization and tacticity. To control these parameters, side-chain liquid crystalline polymers have been synthesized by the living polymerization method, and the relationship between their primary structures and thermotropic phase behaviors has been investigated.

Several research groups have extended the study of the synthesis of block copolymers by using the living polymerization method. They have synthesized block copolymers by cationic,¹ ring-opening metathesis,² and anionic living polymerization,^{3–6} and they reported that these block copolymers displayed liquid crystalline behavior similar to homopolymers and formed a microphase separated structure. On the other hand, other groups have synthesized block copolymers by a polymer reaction using prepolymers,^{7–15} where one block carries functional groups to attach a reactive mesogen. This method is easier than direct living polymerization although the perfect conversion may be generally difficult.

Previously, we synthesized side-chain liquid crystalline poly(methacrylates) with the methoxy biphenyl group as the mesogenic moiety by anionic polymerization at $-40\text{ }^{\circ}\text{C}$.⁴ The resulting polymer had a predictable molecular weight and narrow molecular weight distribution. It exhibited a smectic A mesophase, and the phase transition temperatures increased with the molecular weight. We also synthesized well-defined block copolymers, which contained polystyrene as an amorphous block, by sequential anionic living polymerization.^{4,16,17} The block copolymers formed a lamellar type of microphase separated structure and exhibited the smectic A phase. The lamellar spacing decreased at the

phase change from the crystalline to the isotropic phase after a steady decrease in the smectic A temperature region. The reduction was around 20–25%, which was considered to be caused by the change of the main-chain conformation.^{16,17}

In this paper, we extend the study of the anionic polymerization of 6-[4-(4'-cyanophenyl)phenoxy]hexyl methacrylate (**1**), which has the cyanobiphenyl group



as the mesogenic moiety. Cyanobiphenyl is a typical mesogen, and low molecular weight LC compounds containing the cyano group are often used for display devices. Since cyanobiphenyl is highly reactive with nucleophilic reagents such as carboanion, some research groups synthesized side-chain liquid crystalline polymers containing cyanobiphenyl by other types of living polymerization methods.^{18,19} On the other hand, Ishizone et al. have succeeded in the anionic living polymerization of *p*-cyanostyrene.²⁰ This success suggested the possible extension to monomer **1**. We will present the anionic polymerization of monomer **1** and block copolymerization with methyl methacrylate (MMA) or styrene (St) by sequential polymerization and also examine their thermotropic phase behavior and structures.

2. Experimental Section

The monomer 6-[4-(4'-cyanophenyl)phenoxy]hexyl methacrylate (**1**) was synthesized according to the previous papers.^{4,21} It was dried over P_2O_5 for 48 h under a high vacuum (10^{-6} mmHg), diluted with dry THF to result in 0.05 M solutions, and placed in glass ampules.

Table 1. Anionic Polymerization of 1 in THF for 1 h^a

sample	monomer 1 (mmol)	initiator <i>s</i> -BuLi (mmol)	DPE ^b (mmol)	LiCl (mmol)	temp (°C)	M_n		M_w/M_n^c
						calcd	obsd ^c	
poly(1a)	0.757	0.0278	0.101		−78	10 000	10 000	1.24
poly(1b)	1.18	0.0454	0.0942	0.221	−78	9 400	9 000	1.07
poly(1c)	0.610	0.0386	0.0549	0.165	−40	5 800	6 200	1.09
poly(1d)	1.20	0.0286	0.0475	0.201	−40	15 000	15 000	1.06
poly(1e)	1.31	0.0241	0.0955	0.151	−40	20 000	20 000	1.06

^a Yields of polymers were quantitative. ^b 1,1-Diphenylethylene. ^c M_n (obsd) and M_w/M_n were determined by SEC using the calibration of standard PMMA.

The polymerization of the homopolymers was carried out at −78 to −40 °C with shaking under high-vacuum conditions in an all-glass apparatus equipped with break-seals. After an appropriate polymerization time, the polymerization mixture was poured into methanol to precipitate the polymer. The molecular weight (M_n) and molecular weight distribution (M_w/M_n) were determined by a SEC profile based on the calibration of standard PMMA.

The block copolymers were obtained by the sequential addition of styrene and **1** under similar conditions. The composition of each segment was determined by ¹H NMR. The M_n and M_w/M_n values were estimated from a SEC profile based on the standard polystyrene calibration.

Differential scanning calorimetric (DSC) measurements were carried out with Perkin-Elmer DSC-II at a scanning rate of 10 °C/min. X-ray measurements were carried out by using a Rigaku-Denki X-ray generator with Ni-filtered Cu K α radiation. The fiber specimens were prepared by pulling up the isotropic melt and annealed at the mesophase temperature around 85 °C. The temperatures of the sample were regulated to within 1 °C by using a Mettler FP-82 hot stage. Reflection spacings were calibrated by using a silicon standard. The TEM observation was performed by a Hitachi H-500 transmission electron microscope with a 100 kV accelerating voltage. For this observation, an ultrathin section of the polymer film was prepared as follows. The specimen, after annealed at the mesophase temperature around 85 °C, was dipped in a 1 wt % aqueous solution of ruthenium tetroxide (RuO₄) as the fixing and staining reagent for 20 min. After being dried, the film was embedded in an epoxy resin and cut into ultrathin sections (700–1000 Å thick) by an ultramicrotome with a diamond knife. The sectioned specimens were further stained with the vapor of RuO₄ for 3 min before observation.

3. Results and Discussion

3.1. Anionic Polymerization of Monomer 1. It was considered that the presence of the cyano group of **1** would be a problem for achieving the anionic polymerization of **1**, since the cyano group is not usually compatible with anionic species such as organolithiums and Grignard reagents often used as anionic initiators. However, we have recently demonstrated that cyano-substituted styrene successfully undergoes anionic living polymerization.²⁰ Furthermore, a well-defined tri-block copolymer of poly(MMA-*b*-4-cyanostyrene-*b*-MMA) could be synthesized by the sequential addition of two monomers. These results clearly show that cyano group is sufficiently stable toward living polymer anions derived from 4-cyanostyrene and MMA.

On the basis of the results mentioned above, we first carried out the anionic polymerization of **1** in THF at −78 °C with *s*-BuLi capped with 1,1-diphenylethylene (DPE), which is a typical initiator of alkyl methacrylates. Under such conditions, the polymerization was observed to proceed quantitatively. The chromatogram by SEC showed that the resulting polymer, poly(**1a**), possessed a symmetrical unimodal peak with a relatively narrow molecular weight distribution, an M_w/M_n value being 1.24. Moreover, there is a good agreement

Table 2. Anionic Polymerization of 1 in THF for 1 h^a

sample	monomer 1 (mmol)	initiator (mmol)	additive (mmol)	temp (°C)	M_n		M_w/M_n^b
					calcd	obsd ^b	
poly(1f)	1.40	Ph ₂ CHK ^c 0.0281		−78	18 000	20 000	1.25
poly(1g)	1.41	Ph ₂ CHK 0.0660	ZnEt ₂ ^d 0.375	−78	7 800	8 500	1.10
poly(1h)	1.31	Ph ₂ CHK 0.0417	ZnEt ₂ 0.248	−40	11 000	11 000	1.22
poly(1i)	1.29	Ph ₂ CHK 0.0334	ZnEt ₂ 0.716	−40	14 000	15 000	1.33
poly(1j)	1.42	Ph ₃ CCs ^e 0.0311		−78	17 000	17 000	1.14

^a Yields of polymers were quantitative. ^b M_n (obsd) and M_w/M_n were determined by SEC using the calibration of standard PMMA. ^c Diphenylmethylpotassium. ^d Diethylzinc. ^e Triphenylmethylcesium.

between the M_n values calculated from $[M]/[I]$ and estimated by SEC using PMMA standard samples. These results are summarized in Table 1.

It is observed that the molecular weight distribution is remarkably narrower by the addition of LiCl to the polymerization of **1** (compare poly(**1a**) with poly(**1b**)).²² By changing the **1**-to-initiator ratio, polymers with various molecular weights from 6000 to 20 000, poly(**1b**) to poly(**1e**), were prepared. As can be seen in Table 1, these polymers have narrow molecular weight distributions. The well-controlled polymerization of **1** was maintained by raising the temperature to −40 °C (compare poly(**1b**) with poly(**1c**), poly(**1d**), and poly(**1e**)). These results strongly indicate the living nature of the anionic polymerization of **1** under the conditions employed here. It is obvious that the cyano group is completely stable toward the propagating enolate anion derived from **1** during the course of the polymerization.

The anionic living polymerization of **1** was next carried out with various anionic initiators in THF at −78 °C to examine the scope and possibility of the polymerization of **1**. The initiators used were diphenylmethylpotassium (Ph₂CHK), Ph₂CHK-diethylzinc (Et₂-Zn),²³ and triphenylmethylcesium (Ph₃CCs), which were effective for the polymerization of methyl methacrylate. The results are summarized in Table 2. Ph₂CHK, Ph₂-CHK-Et₂Zn, and Ph₃CCs were found to be effective initiators of the polymerization of **1** in THF at −78 °C. Yields of the polymers were quantitative. The resulting polymers possessed controllable molecular weights and relatively narrow molecular weight distributions, indicating that the polymerization of **1** with each of these initiators also proceeded in a living manner.

The tacticities of the resulting polymers were determined by ¹H NMR according to the literature,^{21,24} in which the three peaks of the α -methyl proton, giving signals at 1.26, 1.07, and 0.94 ppm, were assigned to *mm*, *mr*, and *rr* triads, respectively (see Figure 1). The results are summarized in Table 3. It can be seen that the polymers prepared with the lithium initiator system

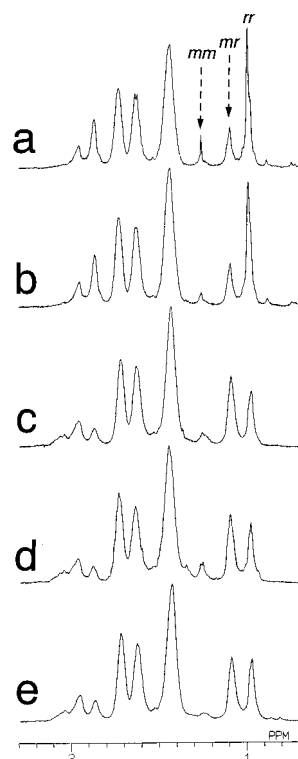


Figure 1. Region of the ^1H NMR spectra showing the peaks associated with the methyl proton (500 MHz, $\text{DMF}-d_7$, 127°C): (a) for poly(**1a**), (b) for poly(**1b**), (c) for poly(**1f**), (d) for poly(**1g**), and (e) for poly(**1j**).

Table 3. Tacticity of Poly(**1**)

run	initiator system	tacticity (%)		
		<i>mm</i>	<i>mr</i>	<i>rr</i>
poly(1a)	<i>s</i> -BuLi/DPE	12	27	61
poly(1c)	<i>s</i> -BuLi/DPE/LiCl	7	26	67
poly(1f)	Ph_2CHK	14	48	38
poly(1g)	$\text{Ph}_2\text{CHK}/\text{Et}_2\text{Zn}$	16	48	36
poly(1j)	Ph_3CCs	7	52	41

have a high syndiotacticity but that the polymers obtained with the potassium and cesium systems are rich in heterotacticity. The additive effect was not observed in the case of either LiCl or Et_2Zn . The dependence of the tacticity of poly(**1**) on the initiator is similar to that observed in the case of PMMA.^{25,26}

3.2. Block Copolymerization. A block copolymer of poly(MMA-*b*-**1**), MMA**1**, was prepared by first the sequential addition of MMA and then **1** in THF at -78°C with *s*-BuLi capped with DPE in the presence of LiCl. As expected, the resulting block copolymer has a predictable molecular weight and a narrow molecular weight distribution, as can be seen in Table 4. Similarly, a well-defined poly(**1**-*b*-MMA), **1MMA**, could be successfully obtained by first the reverse addition of **1** and then MMA under the same conditions. Figure 2 shows the SEC chromatogram of the resulting block copolymer whose peak is unimodal with a narrow distribution of the molecular weight. Furthermore, no peak corresponding to the homopolymer in the first stage is observed as indicated by the arrow in Figure 2. This also provides a direct evidence of the living nature of the polymerization of **1**.

The block copolymer of poly(St-*b*-**1**) was also prepared by the sequential addition of styrene and **1**. In this case, living polystyrene obtained at the first stage was capped with diphenylethylene, followed by the polymerization

Table 4. Block Copolymerization of **1** with Styrene and Methyl Methacrylate at -78°C in THF^a

run	block sequence	M_n		M_w/M_n
		calcd	obsd	
MMA 1	poly(MMA- <i>b</i> - 1) ^b	4800–4900	10 500 ^c	1.04 ^d
1MMA	poly(1 - <i>b</i> -MMA) ^e	8800–9600	18 000	1.06
St 1 -a	poly(St- <i>b</i> - 1) ^f	4600–4700	11 000 (5600–5400) ^g	1.05 ^d
St 1 -b	poly(St- <i>b</i> - 1)	10 000–9000	21 300 (11 700–9600)	1.05
St 1 -c	poly(St- <i>b</i> - 1)	16 000–16 000	36 000 (17 000–19 000)	1.06
St 1 -d	poly(St- <i>b</i> - 1)	31 000–24 000	59 000 (31 000–28 000)	1.03

^a Yields of polymers were quantitative in all runs. ^b Block copolymerization was carried out by sequential addition of MMA with *s*-BuLi, DPE, and LiCl at first and then **1**. Polymerization times at the first and second stage were 10 min and 1 h, respectively. ^c $M_n(\text{obsd})$ and M_w/M_n was determined from SEC profile based on the calibration of standard PMMA. ^d M_w/M_n was determined from SEC profile based on the calibration of standard polystyrene. ^e Block copolymerization was carried out by sequential addition of **1** with *s*-BuLi, DPE, and LiCl at first and then MMA. ^f Block copolymerization was carried out by sequential addition of styrene with *s*-BuLi at first and then **1** after capping with 1,1-diphenylethylene and LiCl. Polymerization times at the first and second stage were 15 min and 1 h, respectively. ^g $M_n(\text{obsd})$ of the poly(**1**) segment was determined by ^1H NMR.

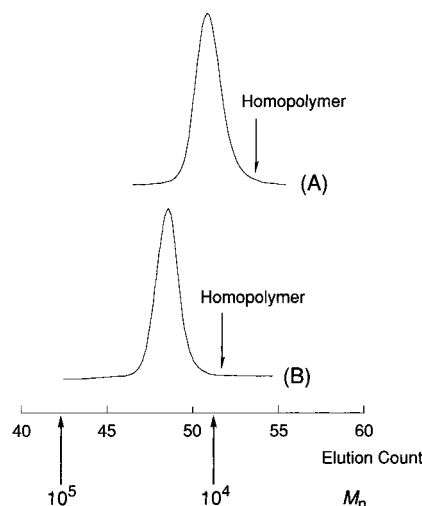


Figure 2. SEC charts of (A) poly(MMA-*b*-**1**) with $M_n = 10\,500$ and $M_w/M_n = 1.04$ and (B) poly(**1**-*b*-MMA) with $M_n = 18\,000$ and $M_w/M_n = 1.06$, which were prepared in sequential polymerization. The arrow indicates the peak position corresponding to the homopolymer synthesized in the first stage.

of **1** in the presence of LiCl in THF at -78°C . As can be seen in Table 4, the resulting block copolymers were satisfactorily regulated with respect to the molecular weight and molecular weight distribution. Four block copolymers, St**1**-a, St**1**-b, St**1**-c, and St**1**-d, were designed here such that the two segments had nearly equal molecular weights, and the whole molecular weights ranged from 10 000 to 60 000.

3.3. Thermotropic Phase Behavior and Structure of Poly(1**).** DSC thermograms of the poly(**1**)s are shown in Figure 3. As can be seen here, all the poly(**1**)s show one dominant peak, which can be assigned to the smectic A (SmA)–isotropic (I) phase transition. No crystallization takes place in this polymeric system, and so the smectic phase glassified on cooling. The temperatures, T_i , and enthalpy changes, ΔH_i , for the SmA–I transition are summarized in Table 5. The glass transition temperatures, T_g , are also given in the same table

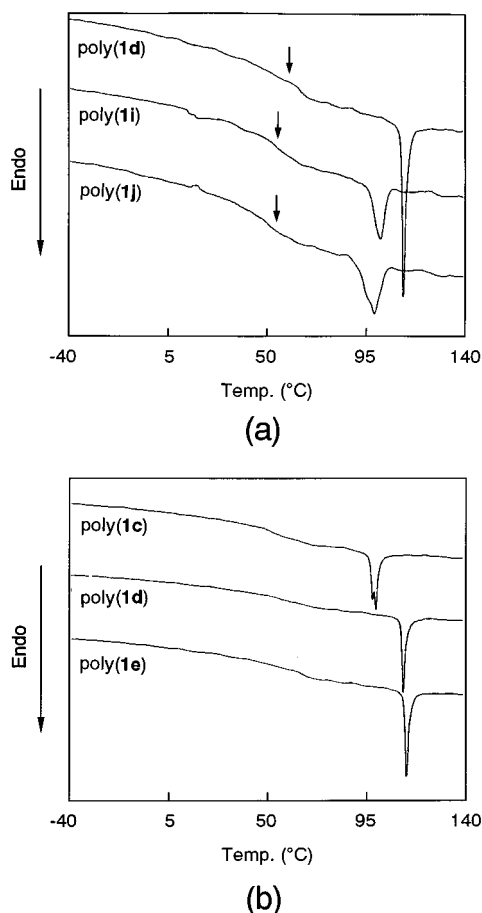


Figure 3. DSC thermograms of the poly(1)s measured at a heating rate of 10 °C/min. One peak observed is attributed to the SmA–isotropic phase transition. The arrow indicates the glass transition. In (a), the DSC thermograms are compared between poly(1d), poly(1i), and poly(1j) with different tacticities, while those in (b) are compared between poly(1c), poly(1d), and poly(1e) with different molecular weights.

Table 5. DSC Data of Poly(1)

sample	countercation	M_n	transition temp, °C (transition enthalpy, kcal/mol)		
			heating		cooling
			T_g	$T_{s-i}(\Delta H)$	$T_{i-s}(\Delta H)$
poly(1c)	Li ⁺	6 200	~60	99.3 (0.49)	97.3 (0.49)
poly(1b)		9 000	~60	103.4 (0.47)	101.3 (0.51)
poly(1a)		10 000	~60	108.2 (0.45)	104.9 (0.43)
poly(1d)		15 000	~60	111.4 (0.48)	109.0 (0.47)
poly(1e)	K ⁺	20 000	~60	113.5 (0.45)	110.9 (0.50)
poly(1g)		8 500	~40	92.5 (0.38)	88.8 (0.31)
poly(1h)		11 000	~50	94.9 (0.43)	90.8 (0.38)
poly(1i)		15 000	~50	102.6 (0.27)	99.7 (0.34)
poly(1f)	Cs ⁺	20 000	~50	101.7 (0.37)	97.5 (0.32)
poly(1j)		17 000	~50	99.8 (0.41)	96.9 (0.38)

although they are roughly estimated because of the broad transition.

We first considered the effect of the tacticity on the transition behavior. In part a of Figure 3, the DSC thermograms are compared between polymers with similar molecular weights but different tacticities. The syndiotactic polymers synthesized via the lithium system show a very narrow peak in comparison with the heterotactic ones synthesized via the potassium and cesium systems. Glass transition temperatures and the SmA–I transition temperatures were also affected by tacticity. Both transition temperatures are relatively

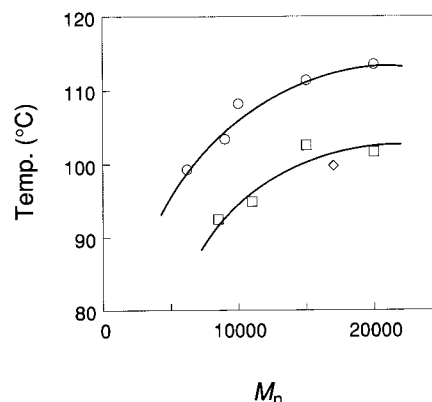


Figure 4. Dependence of the SmA–isotropic phase transition temperature on the molecular weight: (○) Li system, (□) K system, and (◇) Cs system. The transition temperatures are based on a second heating DSC scan.

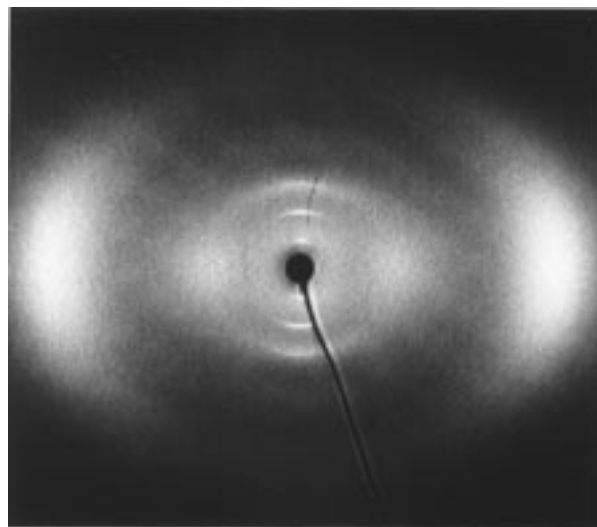


Figure 5. Oriented X-ray patterns of the SmA phase as observed for the fibrous poly(1d). Here, the fiber specimen was prepared by drawing the isotropic melt, and its axis is placed in the vertical direction.

higher in the syndiotactic polymers than in the heterotactic ones. Craig and Imrie have synthesized the same side-chain liquid crystalline polymer by radical polymerization.²¹ The tacticity of the resulting polymer was predominantly heterotactic, and the temperature for the SmA–I transition was 98 °C. The relatively lower T_i corresponds to our data.

The molecular weight also affects the phase transition temperature. This can be seen in part b of Figure 3 where the DSC thermograms are compared between polymers with the same syndiotacticity but with different molecular weights. The SmA–I transition temperatures are plotted as a function of M_n in Figure 4. In both the syndiotactic and heterotactic systems, the isotropization temperature increases with the increase in molecular weight and levels off at an M_n more than 15 000.

Figure 5 shows the X-ray pattern observed for the oriented SmA of poly(1d), which was prepared as a fiber by pulling from the isotropic melt. In this pattern, there are three inner reflections along the meridian as well as an outer broad reflection along the equator. The smectic layer is thus oriented perpendicularly to the fiber axis. The layer spacing estimated is 36.0 Å. This value is somewhat larger than the layer spacing of 26.6

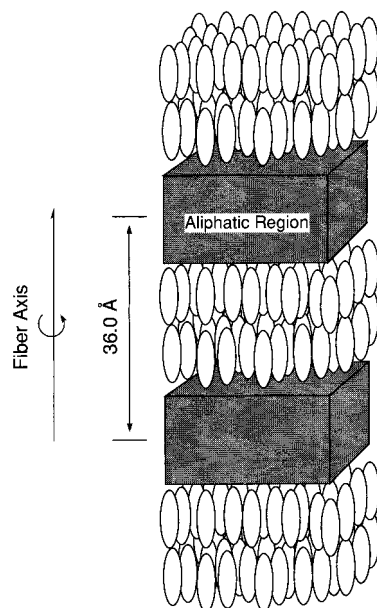


Figure 6. Schematic illustration of the plausible layered structure in the fibrous SmA phase.

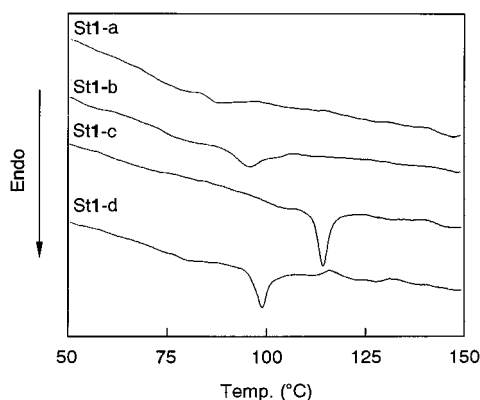


Figure 7. DSC thermograms of the block copolymers with polystyrene segment measured at a heating rate of 10 °C/min: (a) St1-a, (b) St1-b, (c) St1-c, and (d) St1-d. One peak observed is due to the SmA–isotropic phase transition of the poly(1) segment.

Å of the poly[6-[4-(4'-methoxyphenyl)phenoxy]hexyl methacrylate]⁴ with a methoxy end group and is comparable to twice the side-chain length (21.3 Å) in its fully extended form. The smectic layers are thus constructed with a bilayer character in which two mesogenic layers are included within a repeat length. Such a bilayer formation is typical for cyanobiphenyl mesogens.²⁷ The tentative layer structure is illustrated in Figure 6. It should be noted here that molecular weight and tacticity do not affect such structural characteristics of the smectic phase.

3.4. Thermotropic Phase Behavior and Structure of Block Copolymers. The two block copolymers with PMMA (MMA1 and 1MMA) show no significant DSC peaks. X-ray and TEM observations also show only a poorly ordered microphase separation, for which we cannot give a reasonable answer at this time.

On the other hand, the block copolymers of poly(St-*b*-1) exhibit one dominant transition similar to the homopolymers (see Figure 7). The thermodynamic data are listed in Table 6. The phase sequence is also similar, i.e., SmA glass–SmA–I. The block copolymer with the microphase separation should exhibit two glass transi-

Table 6. DSC Data of Poly(St-*b*-1)

sample	transition temp, °C (transition enthalpy, kcal/mol ^a)	
	heating	cooling
St1-a	87.6 (0.09)	84.8 (0.04)
St1-b	96.4 (0.27)	92.0 (0.25)
St1-c	114.5 (0.30)	111.7 (0.30)
St1-d	99.2 (0.29)	95.1 (0.29)

^a Transition enthalpy as estimated per mole of poly(1) segment.

tions, but in this system the individual glass transition temperature could not precisely be determined because the two glass transitions are too small and close to each other.

The SmA–I transition peak of poly(St-*b*-1)s is broader and the transition enthalpy is significantly smaller when they are evaluated per the poly(1) segment (compare Tables 5 and 6). This tendency was also observed in our previous works^{4,16} and other groups' works^{2,3,6–15} and explained as resulting from the disordering of the SmA structure near the microphase interface.

Figure 8 represents TEM photographs as observed for the poly(St-*b*-1)s. It clearly demonstrates the microphase separation, where the liquid crystalline poly(1) microdomains appear dark because of the staining with RuO₄.⁴ For St1-a, St1-b, and St1-d among the four poly(St-*b*-1) copolymers, the basic morphologies are of the lamellar type as expected from the weight fraction of the block copolymers being around 50% (see Figure 8a,b,d). On the other hand, the St1-c sample shows the cylindrical type of microphase separation, where the cylinder part is composed of the poly(1) segments (Figure 8c). The lamellar microphase structure for St1-a, St1-b, and St1-d and the cylindrical microphase structure for St1-c can also be clarified from small-angle X-ray profiles as shown in Figure 9. The reflection spacings elucidated are collected for all the specimens in Table 7.

To obtain information about the relationship between the microphase separated structure and liquid crystalline structure, the oriented specimen was analyzed by a coupling of wide-angle X-ray (WAXD) and small-angle X-ray (SAXS) methods. Parts a and b of Figure 10 show WAX patterns for the SmA phases in the fiber specimen of St1-b and St1-c, respectively. Here, the fiber was prepared by pulling up the isotropic melt and placed in a vertical direction. The layer reflections can be observed on the meridional, and their spacings coincide with those observed in the homopolymer. Parts c and d of Figure 10 show SAX patterns of St1-b and St1-c, respectively. The reflections of the microphase separation were observed along the equator, and hence, the lamellae of St1-b and the cylinders of St1-c are oriented parallel to the fiber direction. From a comparison of these results, the schematic illustration of plausible layer structures in the fibrous specimens of St1-b and St1-c are shown in Figure 11, where the mesogenic groups lie parallel to the interface of the domains. A similar orientation trend has been observed by Gronski et al.,^{7,13} Fischer et al.,^{10–12} Ober et al.,¹⁴ and Yamada et al.,^{4,16,17} although the unexpected orientation is also reported by Hammond et al.²⁸

Keeping these structures in mind, it is interesting to note that the SmA–I transition is sharper and its temperature is higher for St1-c than for St1-a, St1-b, and St1-d (see Table 6 and Figure 7). This means that

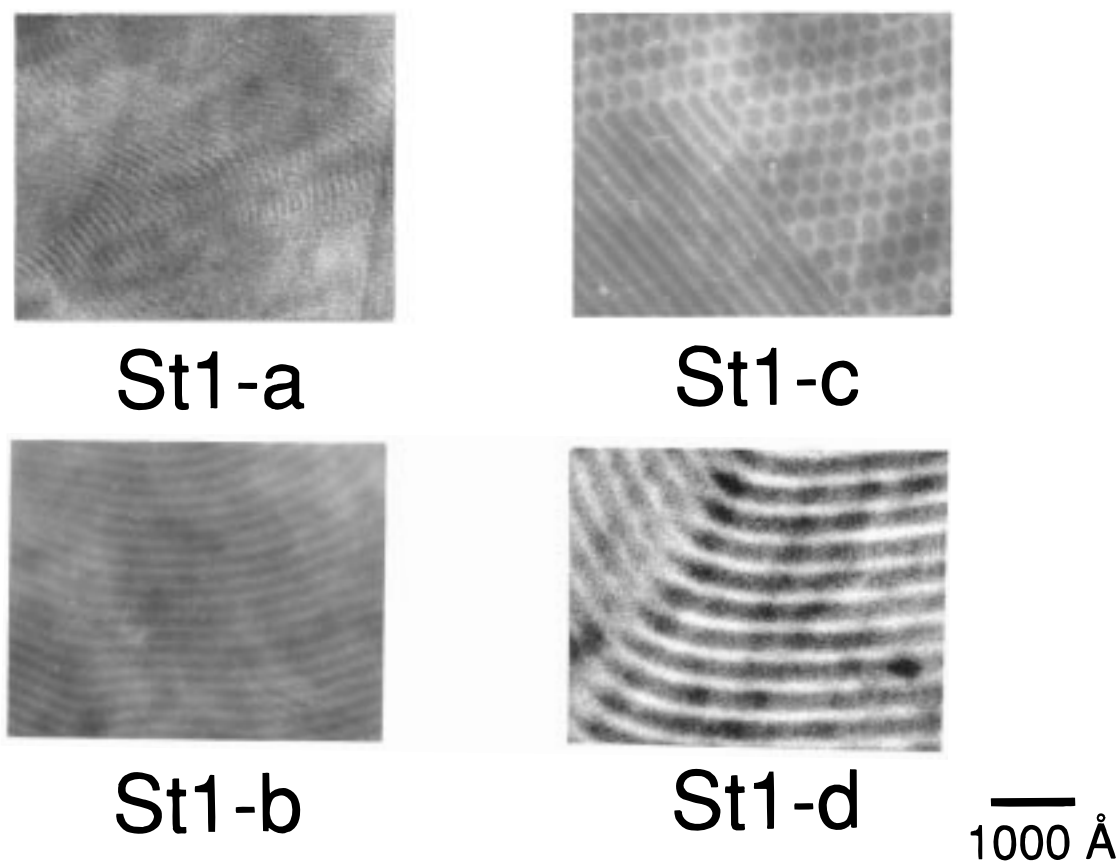


Figure 8. TEM photographs observed for the ultrathin sections of the block copolymers with polystyrene: (a) St1-a, (b) St1-b, (c) St1-c, and (d) St1-d.

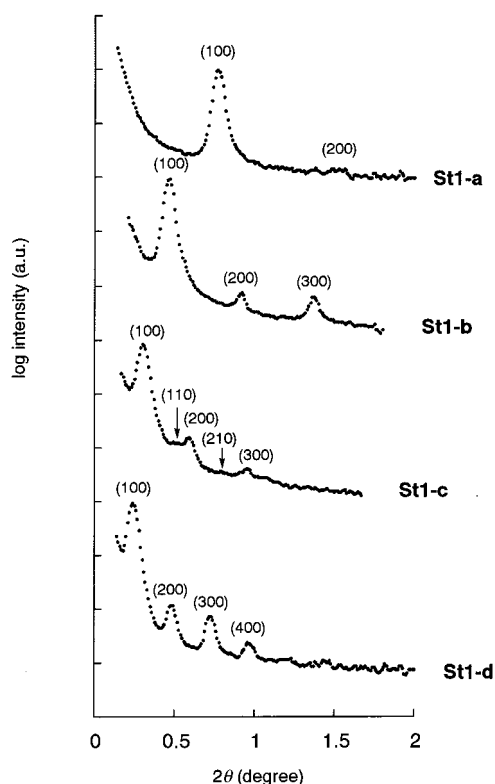


Figure 9. SAXS intensity profiles of block copolymers with polystyrene: (a) St1-a, (b) St1-b, (c) St1-c, and (d) St1-d.

the mesogenic groups are packed more efficiently in the cylindrical domain than in the lamellar domain. The reason for this, as well as the reason why only St1-c

Table 7. Lamellar Spacings (Å) of the Poly(St-*b*-1)

sample	lamellar spacing (Å)
St1-a	115
St1-b	194
St1-c	(291) ^a
St1-d	353

^a (100) reflection from cylindrical microdomain.

takes up the cylindrical microphase separation, is under consideration.

The SAX measurements were carried out at a variety of temperatures. In the block copolymer systems with the methoxy biphenyl moiety as mesogen, the lamellar spacing decreased significantly in the temperature range of the SmA phase; the overall change in the lamellar spacing was as large as one-fifth of the lamellar spacing.^{16,17} The reduction is considered to be caused by the change of the main-chain conformation from the extended form to the random coil conformation. On the other hand, a definitive change of spacing was not observed through the SmA glass–SmA–I phases in the poly(St-*b*-1) specimens (see Figure 12), suggesting that the main-chain conformation in the smectic phase is not significantly altered from that in the isotropic phase. Such two distinct trends in temperature dependence of the lamellar spacing may be attributable to the structural difference in the SmA phases between the two copolymer systems. A detailed examination is proceeding now on this point.

4. Conclusion

We have performed the anionic living polymerization of 6-[4-(4'-cyanophenyl)phenoxy]hexyl methacrylate and

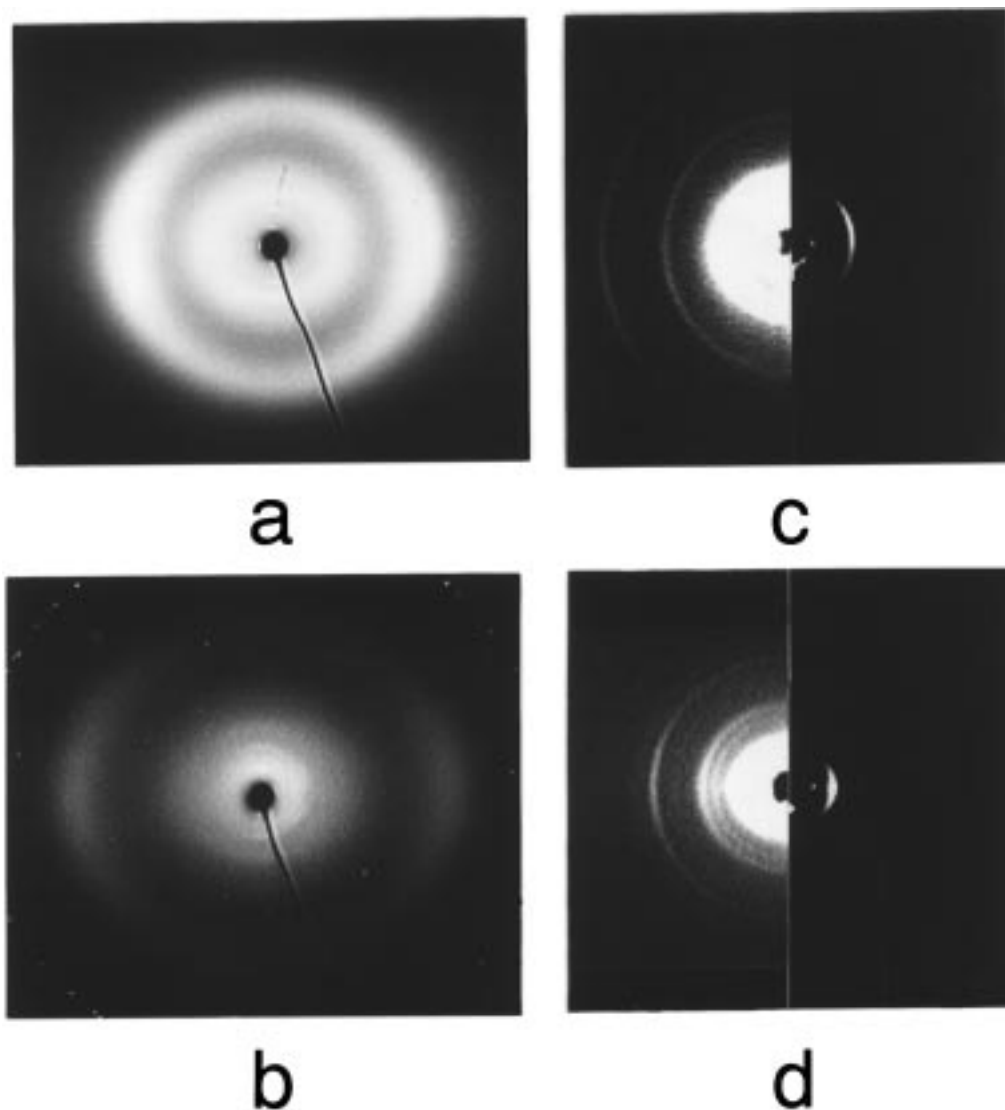


Figure 10. Wide-angle X-ray patterns of (a) St1-b and (b) St1-c and small-angle X-ray patterns of (c) St1-b and (d) St1-c. The X-ray patterns were taken in the smectic temperature region for the fiber specimens that were prepared by drawing the isotropic melt. The fiber axes are in the vertical direction.

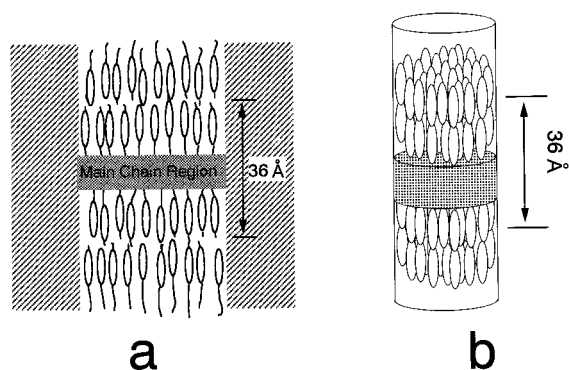


Figure 11. Schematic illustration of smectic layers within the microdomain of fibrous block copolymer as elucidated from the X-ray data in Figure 10: (a) St1-b with the lamellar microdomain and (b) St1-c with the cylindrical microdomain. block copolymerization with MMA and styrene. By the choice of suitable initiation, it was found that the cyano group is completely stable toward the propagating enolate anion during the course of the polymerization and that the anionic polymerization proceeds with the living nature. The homopolymers were prepared with a wide range of molecular weights from 6000 to 20 000,

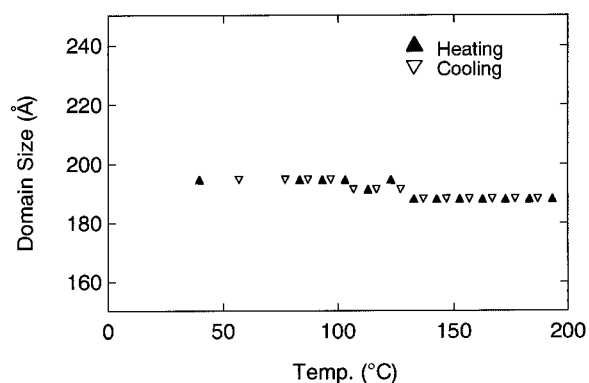


Figure 12. Temperature dependence of the lamellar spacing in the microphase segregation structure as observed in St1-b.

narrow molecular weight distributions, and different tacticities. All the polymers exhibited the SmA phase in which the two mesogenic layers were included in a layer with a thickness of 36.0 Å. No crystallization took place so that the SmA phase was glassified on cooling. The isotropization temperature of the SmA phase increased with an increase in the molecular weight and leveled off at M_n of more than 15 000. Syndiotactic

polymers showed relatively sharper transitions and higher transition temperatures than the heterotactic polymers.

The block copolymers with MMA and styrene were also prepared successfully by living anionic polymerization. The well-defined microphase segregation was observed in the block copolymers with styrene, poly(St-*b*-1)s. For three of the poly(St-*b*-1) samples with the molecular weights of two segments, PSt/poly(1) = 5 600/5400, 11 700/9600, and 31 000/28 000, the microphase separation was found to be of the lamellar type, while the copolymer with 17 000/19 000 showed the cylinder type of microphase separation in which the cylinder part consisted of the poly(1) segment. We are now proceeding with the study to clarify the reason why the type of morphology depends on the molecular weight. For all the poly(St-*b*-1)s, the thermotropic phase behavior is similar to that in homopolymer. No detectable temperature dependence of the domain size was observed. This dependence is remarkably different from that in the block copolymers based on 6-[4-(4'-methoxyphenyl)-phenoxy]hexyl methacrylate previously reported, suggesting that the main-chain conformation is not significantly altered through the SmA glass-SmA-isotropic phases.

References and Notes

- (1) Percec, V.; Lee, M. *Pure Appl. Chem.* **1992**, A29, 723.
- (2) Komiya, Z.; Schrock, R. R. *Macromolecules* **1993**, 26, 1387.
- (3) Bohnert, R.; Finkelmann, H. *Macromol. Chem. Phys.* **1994**, 195, 689.
- (4) Yamada, M.; Iguchi, T.; Hirao, A.; Nakahama, S.; Watanabe, J. *Macromolecules* **1995**, 28, 50.
- (5) Zheng, W. Y.; Hammond, P. T. *Macromol. Rapid. Commun.* **1996**, 17, 813.
- (6) Zheng, W. Y.; Hammond, P. T. *Macromolecules* **1998**, 31, 711.
- (7) Adams, J.; Gronski, W. *Makromol. Chem., Rapid Commun.* **1989**, 10, 553.
- (8) Zschke, B.; Frank, W.; Fischer, H.; Schmtzler, K.; Arnold, M. *Polym. Bull.* **1991**, 27, 1.
- (9) Arnold, M.; Poser, S.; Fischer, H.; Frank, W.; Utschick, H. *Macromol. Rapid Commun.* **1994**, 15, 487.
- (10) Fischer, H.; Poser, S.; Arnold, M.; Frank, W. *Macromolecules* **1994**, 27, 7133.
- (11) Fischer, H.; Poser, S.; Arnold, M. *Liq. Cryst.* **1995**, 18, 503.
- (12) Fischer, H.; Poser, S.; Arnold, M. *Macromolecules* **1995**, 28, 6957.
- (13) Adams, J.; Sanger, J.; Tefehne, C.; Gronski, W. *Macromol. Rapid Commun.* **1994**, 15, 879.
- (14) Mao, G.; Wang, J.; Clingman, S. R.; Ober, C. K.; Chen, J. T.; Thomas, E. L. *Macromolecules* **1997**, 30, 2556.
- (15) Sanger, J.; Gronski, W.; Maas, S.; Stuhn, B.; Heck, B. *Macromolecules* **1997**, 30, 6738.
- (16) Yamada, M.; Iguchi, T.; Hirao, A.; Nakahama, S.; Watanabe, J. *Polym. J. (Tokyo)* **1998**, 30, 23.
- (17) Yamada, M.; Itoh, T.; Hirao, A.; Nakahama, S.; Watanabe, J. *High Perform. Polym.* **1998**, 10, 131.
- (18) Percec, V.; Tomazos, D. *Adv. Mater.* **1992**, 4, 548.
- (19) Komiya, Z.; Schrock, R. R. *Macromolecules* **1993**, 26, 1393.
- (20) Ishizone, T.; Sugiyama, K.; Hirao, A.; Nakahama, S. *Macromolecules* **1993**, 26, 3009.
- (21) Craig, A. A.; Imrie, C. T. *Macromolecules* **1995**, 28, 3617.
- (22) Fayt, A.; Forte, R.; Jacobs, C.; Jerome, R.; Ouhadi, T.; Teyssie, Ph.; Varshney, S. K. *Macromolecules* **1987**, 20, 1442.
- (23) Ozaki, H.; Hirao, A.; Nakahama, S. *Macromol. Chem. Phys.* **1995**, 196, 2099.
- (24) Nakano, T.; Hasegawa, T.; Okamoto, Y. *Macromolecules* **1993**, 26, 5494.
- (25) Long, T. E.; Allen, R. D.; McGrath, J. E.; In, *Recent Advances in Mechanistic and Synthetic Aspects of Polymerization*; Fontanille, M.; Guyot, A., Eds.; NATO ASI Ser. C; Plenum: New York, 1987; Vol. 215, p 79.
- (26) Hatada, K.; Sugino, H.; Ise, H.; Kitayama, T.; Okamoto, Y.; Yuki, H. *Polym. J. (Tokyo)* **1980**, 12, 55.
- (27) McArdle, C. B. *Side Chain Liquid Crystal Polymers*; Chapman and Hall: New York, 1989; Chapter 3.
- (28) Zheng, W. Y.; Albalak, R. J.; Hammond, P. T. *Macromolecules* **1998**, 31, 2686.

MA981366N